

Acoustics between a Shock and a Contact Surface - Relevance to Galloping Detonations

Luc Bauwens
The University of Calgary
Department of Mechanical and Manufacturing Engineering
2500 University Drive NW
Calgary, AB T2N 1N4, Canada
bauwens@ucalgary.ca

Keywords: Galloping detonations, Newtonian limit, acoustics, Riemann problem

Acoustics between a leading shock and a contact surface play a role in a number of scenarios relevant to initiation, failure and propagation of detonations. This includes piston-initiated ignition, which has been studied in the Newtonian limit by Blythe and Crighton (1989), and the related problem of hot spot formation between a shock and a contact surface resulting from shock collision (Short and Dold 1996). Propagation of low overdrive one-dimensional detonations can be described as a sequence of failure and reignitions, and the reignition scenario is very similar to the ignition problem (Bauwens et al. 1998). The difference between these various scenarios is characterized by the reflection coefficient at the contact surface (Bauwens 1999). But these various scenarios also differ in a second aspect, which is of concern here: whether resonant acoustics plays a role. The studies of the piston-initiated ignition problem (Blythe and Crighton 1989) and of the shock collision problem (Short and Dold 1996) were formulated as initial value problems with clean initial conditions, effectively setting the amplitude of resonant acoustics to zero.

But there are other circumstances, for instance when stability is an issue, or in the processes subsequent to failure, when the reaction zone becomes decoupled from the leading shock, and where a non-trivial decaying flow will feed into the acoustics. In the failure and reignition scenario, decay subsequent to failure clearly will leave behind a non-homogeneous acoustic initial condition, although on much shorter length- and time scales than reignition, which is controlled by slow chemistry. Likewise, in numerical simulations, the numerical error will feed into any physical resonance inherent to the problem being solved.

On a domain that initially has zero length but increases at a constant rate, the resonant acoustic problem is a self-similar Riemann problem to arbitrary magnitude less than unity, with eigensolutions given by power laws in the invariants, with complex exponents that depend upon the reflection coefficients at the ends, and with a decaying real part, hence an initial singularity. Here, the problem is formulated in the Newtonian limit $\gamma - 1 \ll 1$; this has little effect on the formulation besides allowing for decoupling resonant acoustics from the heat release even if the magnitude of the resonant acoustics is the same as the effect of slow chemistry. The index 0 is used for the leading order solution, which is uniform, and u , p , with no index are the velocity and pressure perturbations; x and t are the space and time coordinate, based upon the slow chemical time. The problem can be written as:

$$p_0 \frac{\partial u}{\partial t} + p_0 u_0 \frac{\partial u}{\partial x} + \frac{\partial p}{\partial x} = 0 \quad \frac{\partial p}{\partial t} + u_0 \frac{\partial p}{\partial x} + p_0 \frac{\partial u}{\partial x} = 0 \quad (1a,b)$$

Assuming radiating boundary conditions downstream (see for instance the discussion in Lee and Stewart 1990), the boundary conditions can be expressed as pressure reflection coefficients, F_S at the contact surface and F_C at the shock. θ being the temperature ratio across the contact surface and M , the shock Mach number, these are:

$$F_C = \frac{1 - \sqrt{\theta}}{1 + \sqrt{\theta}} \quad F_S = -\frac{(M - 1)^2}{(M + 1)^2} \quad (2a,b)$$

Using the notation $z_R = t + u_0 t - x$ and $z_L = t - u_0 t + x$, the solution can then be written as a right- and a left-going wave, satisfying Eqs. (1a,b):

$$\frac{p}{p_0} = R(z_R) + L(z_L) \quad \text{and} \quad u = R(z_R) - L(z_L) \quad (3a,b)$$

in which the functions $R(z_R)$ and $L(z_L)$ are determined by the boundary conditions: $R(z) = F_S L(z\sqrt{-F_S})$ and $L(z) = F_C R(z)$. This yields a solution of the form $R(z) = K z^m$, with m determined by the dispersion relation

$$1 = -F_C (-F_S)^{1+m/2} \quad (4)$$

Then, for F_S and F_C negative, writing $m = -\eta + i\omega$, and with $k = 0, 1, 2, 3, \dots$

$$\eta = 2 + 2 \frac{\log(-F_C)}{\log(-F_S)} \quad \text{and} \quad \omega_k = \frac{-4k\pi}{\log(-F_S)} \quad (5a,b)$$

and since both reflection coefficients have values between -1 and zero, both η and ω are positive and a nonoscillatory mode exists for $k = 0$. This is no longer the case if F_C positive, when

$$\eta = 2 + 2 \frac{\log F_C}{\log(-F_S)} \quad \text{and} \quad \omega_k = \frac{-2(1+2k)\pi}{\log(-F_S)} \quad (6a,b)$$

And in both cases, the solution can be written as

$$R(z) = \sum_{k=0}^{\infty} K_k z^{-\eta+i\omega_k} \quad \text{and} \quad L(z) = F_C \sum_{k=0}^{\infty} K_k z^{-\eta+i\omega_k} \quad (7a,b)$$

Thus, returning to real form, and combining the left- and right-going modes, pressure and velocity include terms such as $(t + u_0 t - x)^{-\eta} \sum_{k=0}^{\infty} A_k \cos[\omega_k \log(t + u_0 t - x) + \phi_k]$ and $(t - u_0 t + x)^{-\eta} \sum_{k=0}^{\infty} A_k \cos[\omega_k \log(t - u_0 t + x) + \phi_k]$.

Introducing the similarity variable $\xi = x/t$, so that $z_L = t(1 - u_0 + \xi)$ and $z_R = t(1 + u_0 - \xi)$, the solution becomes

$$\frac{p}{p_0} = t^{-\eta} \sum_{k=0}^{\infty} K_k t^{i\omega_k} \{ (1 + u_0 - \xi)^{-\eta+i\omega_k} + F_C (1 - u_0 + \xi)^{-\eta+i\omega_k} \} \quad (8a)$$

$$u = t^{-\eta} \sum_{k=0}^{\infty} K_k t^{i\omega_k} \{ (1 + u_0 - \xi)^{-\eta+i\omega_k} - F_C (1 - u_0 + \xi)^{-\eta+i\omega_k} \} \quad (8b)$$

Both amplitude **and frequency** decay as a power law with exponent $-\eta$, and η , given by Eq. (5a) or Eq. (6a), has a value of approximately 3. Physically, this behavior results from wave reflections between two boundaries, the shock and the contact surface, which move away from each other, so that the time interval between reflections increases linearly. Furthermore, if both reflection coefficients are negative, then a nonoscillatory mode is possible, because reflections at both ends entail a sign change, so that after the two reflections the same sign is recovered. While the reflection coefficient at the shock, F_S , is always negative, at the contact surface, F_C , given by Eq. (2a), is negative only if the temperature downstream is higher than in the interval between shock and contact surface. Thus a nonoscillatory mode will exist in these scenarios where the contact surface represents a flame (with propagation speed negligible compared with the speed of sound) or following failure, but not in milder scenarios such as piston-initiated ignition. The non-oscillatory mode results in pressure and velocity given by:

$$\frac{p}{p_0} = K_0 \{ (t + u_0 t - x)^{-\eta} + F_C (t - u_0 t + x)^{-\eta} \} \quad (9a)$$

$$u = K_0 \{ (t + u_0 t - x)^{-\eta} - F_C (t - u_0 t + x)^{-\eta} \} \quad (9b)$$

The complex coefficients $\{K_k\}$ are determined by the initial conditions. In the case of the failure process, which occurs on the short time scale $\tau_N = k\beta \exp \{ [1 - (\gamma - 1)T_{11N}]/\beta \}$, with T_{11N} representing the temperature contribution of order $\gamma - 1$ evaluated at the Neumann point of the original detonation before failure, and β representing the inverse dimensionless activation energy. These modes initially contribute to a nonzero flow of

order $\beta/(\gamma - 1)$, which will shift the location of the hot spot by a distance of order $\exp [-(\gamma - 1)/\beta]$, overwhelming the effect of compressibility on the hot spot location (Bauwens 1999) if $(\gamma - 1)^2 \ll \beta$.

From a stability standpoint, including numerical models, these modes, which decay very quickly, may seem harmless. They do, however, result in frequencies which are initially very high compared with the (re)ignition time, although they are limited by the chemical time in the reaction zone before failure. Still, in low overdrive galloping detonations, very large explosions may occur (see for instance Williams et al. 1996), in which the chemical time is very small. Figure (1) (taken from Williams et al. 1996) shows the pressure behind the leading shock, vs. time, from a one-dimensional computation of a low overdrive galloping detonation. The picture shows the sequence of events triggered by a large explosion. A large explosion, in which pressures of about four times the downstream pressure of a steady ZND detonation in the same regime, comes from downstream and hits the leading shock at $t = 234$. This is followed by extinction. Superimposed on a mean pressure that decreases monotonically at a rate close to $t^{-\eta}$, oscillations occur, with shape exhibiting sharp peaks and shallow troughs, and the period increases sharply in time, although the amplitude does not appear to behave in any predictable way. But clearly, one cannot expect the linearized acoustic model to predict quantitatively the initially strongly nonlinear regime. Furthermore, since the grid sizes used in computations are finite, it is unlikely that the very high frequencies that occur initially can be adequately resolved, and the amplitude of the highest frequencies that appear on the figure is most likely underestimated, which is probably why high amplitudes are noted only later in the process. Still, the global rate of decay and the decrease in frequency appear to be consistent with a scenario in which reflections with a sign change occur both at the shock and the contact surface.

References:

- Bauwens, L., "Ignition between a Shock and a Contact Surface with Arbitrary Reflection Coefficient," paper No. 38, 17th ICDERS (1999).
- Bauwens, L., Williams D.N. and Nikolic, M., *27th International Symposium on Combustion*, The Combustion Institute, Pittsburgh, PA (1998).
- Blythe, P.A. and Crighton, D.G., *Proc. R. Soc. Lond. A* **426**:189-209 (1989).
- Lee H.I. and Stewart D.S., *J. Fluid Mech.* **216**: 103-132 (1990).
- Short, M. and Dold, J.M., *SIAM J. Appl. Math.* **56**:1295-1316 (1996).
- Williams, D.N., Bauwens, L. & Oran, E.S., *Shock Waves* **6**:93-110 (1996).

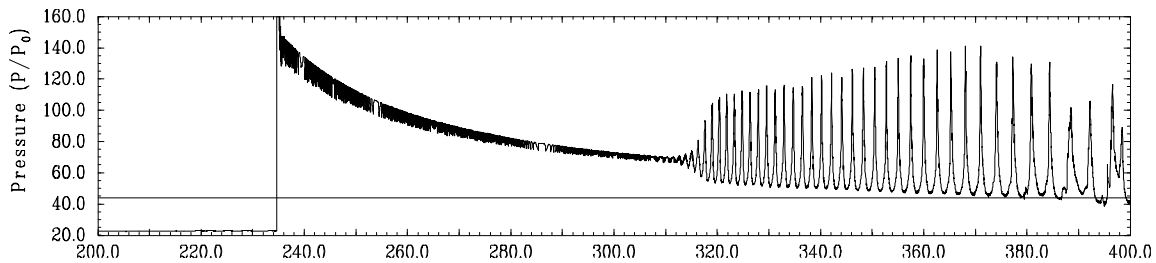


Fig. 1. Pressure behind leading shock (Williams et al. 1996)